NATIONAL ADVISORY COMMITTEE FOR AERONAUTICS

TECHNICAL NOTE

No. 1377

WIND-TUNNEL INVESTIGATION OF UNSHIELDED HORN BALANCES ON A HORIZONTAL TAIL SURFACE

By John G. Lowry and Stewart M. Crandall

Langley Memorial Aeronautical Laboratory
Langley Field, Va.

Washington
July 1947

NATIONAL ADVISORY COMMITTEE FOR AERONAUTICS

TECHNICAL NOTE NO. 1377

WIND-TUNNEL INVESTIGATION OF UNSHIELDED HORN BALANCES ON A HORIZONTAL TAIL SURFACE

By John G. Lowry and Stewart M. Crandall

SUMMARY

A wind-tunnel investigation has been made to determine the aerodynamic characteristics of a horizontal tail surface with various amounts of unshielded horn balance and with the surface condition similar to that of a typical fabric-covered elevator.

The wind-tunnel results indicated that the increments for the variation of hinge-moment coefficient with angle of attack and elevator deflection caused by change in the size of the unshielded horn are approximately linear functions of the ratio of the horn area moment to the elevator area moment. The control-force characteristics as estimated from the wind-tunnel data and as obtained from flight tests were in good agreement when the surface irregularities of the airplane were simulated on the model.

INTRODUCTION

An investigation has been made in the Langley 7- by 10-foot tunnel and in flight of the horizontal tail surface of a torpedo bomber. Preliminary flight tests of the airplane showed that a large undesirable change in trim force occurred when the flaps were extended and that the maneuvering forces were excessive. The wind-tunnel investigation was undertaken to determine the aerodynamic characteristics of the tail surface with various amounts of unshielded horn balance so that a satisfactory configuration could be determined. The variations consisted of removing part of the unshielded horn and adding it to the stabilizer. Flight tests of one arrangement were made to corroborate the wind-tunnel results.

The present paper gives only the details of the wind-tunnel investigation. The control characteristics obtained in flight are compared with those estimated from wind-tunnel data.

METHODS AND APPARATUS

The test setup is shown schematically in figure 1 and in the photograph of figure 2. The semispan model was mounted vertically in the Langley 7- by 10-foot tunnel with the inboard end adjacent to the tunnel floor which thereby acted as a reflection plane. The model was supported entirely by the balance frame with a small clearance at the tunnel floor so that all forces and moments acting on the model could be measured. The flow over the model simulated the flow over the left semispan of a complete horizontal tail mounted in a 10- by 14-foot tunnel. Provisions were made for changing the angle of attack of the model and the deflection of the elevator while the tunnel was in operation. Elevator hinge moments were measured by means of an electrical strain gage mounted within the elevator. No tab hinge moments were recorded.

The 0.5-scale model of a left horizontal tail surface was furnished by the manufacturer and conformed to the dimensions given in figure 3. Geometric characteristics of the model and the airplane are given in table I. The model represented the part of the airplane crosshatched in figure 4.

Four different amounts of horn were tested on the model (fig. 5). In these variations of the horn, strips about 1.5 inches wide were cut from the horn and added to the stabilizer. The gap between the outboard end of the stabilizer and the horn was kept at a constant value of 0.25 inch.

Certain modifications were made to the elevator during the tests which made the model more nearly represent the horizontal tail surface of the particular airplane flight tested. The details of the modifications are shown in figures 5 to 7. Modification A consisted of enlarging the gap between the stabilizer and elevator by replacing the circular trailing-edge section of the stabilizer (fig. 3) with a channel section (fig. 5). Modification B included modification A and in addition consisted of enlarging the cut-out for the hinge-moment device to correspond to the tab mechanism cut-out on the airplane. Modification C included modifications A and B and an alteration of the elevator to simulate the contour and surface irregularities of the fabric-covered elevator on the airplane (figs. 6 and 7).

A dynamic pressure of 16.37 pounds per square foot was maintained for all tests and corresponds to a velocity of approximately 80 miles per hour and to a test Reynolds number of 1,920,000 based on the model mean chord of 2.63 feet.

COEFFICIENTS

C_L lift coefficient (L/qS)

C_D drag coefficient (D/qS)

C_m pitching-moment coefficient (M/qSc')

C_h elevator hinge-moment coefficient $(H_e/qb_e\bar{c}_e^2)$

where

L twice lift of semispan model

D twice drag of semispan model

M twice pitching moment of semispan model about mounting axis (fig. 3)

H_e twice elevator hinge moment of semispan model

q dynamic pressure $\left(\frac{1}{2}\rho V^2\right)$

S twice area of semispan model

b_e twice elevator span of semispan model

c' mean chord of semispan model

$\bar{c}_e$ root-mean-square chord of elevator

and

ρ mass density of air

V free-stream velocity

V_i indicated airspeed

α angle of attack, degrees

δ_e elevator deflection relative to stabilizer, positive when trailing edge is deflected downward

δ_t tab deflection relative to elevator, positive when trailing edge is deflected downward

c_e elevator chord, inches

c_t tab chord, inches

F_s stick force, pounds

$\frac{\partial \epsilon}{\partial \alpha}$ rate of change of downwash angle at tail of airplane with airplane angle of attack

n normal acceleration during maneuvers, g units

M_e elevator area moment behind hinge axis about elevator hinge axis

M_h horn area moment about elevator hinge axis (fig. 3)

$\frac{\Delta C_{h_{curves}}}{\Delta C_{h_{slopes}}}$ ratio of increment of hinge-moment coefficient obtained from curves of plotted data to increment obtained from slopes of hinge-moment curves measured at $\alpha = \delta_e = 0^\circ$

$$C_{L_\alpha} = \left(\frac{\partial C_L}{\partial \alpha}\right)_{\delta_e, \delta_t}$$

$$C_{L_{\delta_e}} = \left(\frac{\partial C_L}{\partial \delta_e}\right)_{\alpha, \delta_t}$$

$$C_{h_\alpha} = \left(\frac{\partial C_h}{\partial \alpha}\right)_{\delta_e, \delta_t}$$

$$C_{h_{\delta_e}} = \left(\frac{\partial C_h}{\partial \delta_e}\right)_{\alpha, \delta_t}$$

$$C_{L_{\delta_t}} = \left(\frac{\partial C_L}{\partial \delta_t}\right)_{\alpha, \delta_e}$$

$$C_{h_{\delta_t}} = \left(\frac{\partial C_h}{\partial \delta_t}\right)_{\alpha, \delta_e}$$

$$\alpha_{\delta_e} = \left(\frac{\partial \alpha}{\partial \delta_e}\right)_{C_L, \delta_t}$$

CORRECTIONS

Jet-boundary corrections were obtained by the methods of reference 1 and were applied to all the data as follows:

$$\Delta\alpha = 1.48C_L$$

$$\Delta C_D = 0.0235C_L^2$$

$$\Delta C_m = 0.0069C_L$$

$$\Delta C_h = 0.0053C_L$$

No corrections have been made for the effect of the gap between the root section and the floor or leakage around the support strut.

PRESENTATION OF DATA

Results of the tests of various horns, elevator modifications, and tab settings are presented in figures 8 to 20. Figure 21 illustrates the variation of C_{h_α} and $C_{h_{\delta_e}}$ as a function of the ratio of horn area moment to elevator area moment. A comparison of the curves of C_h against δ_e for the various horns is presented in figure 22. Figure 23 gives for one of the modified tail surfaces a comparison of the longitudinal trim characteristics estimated from wind-tunnel data with the trim characteristics obtained in flight.

DISCUSSION

Hinge-Moment Characteristics

The results of both wind-tunnel and flight tests with the original elevator (see tabulated stick forces in table II) indicate that it is necessary for the model to represent the tail surface of the airplane as nearly as possible if correlation with flight tests is to be expected. A summary (table II) of the parameters obtained from the wind-tunnel tests (figs. 8 to 20) shows that the original model gave values of C_{h_α} and $C_{h_{\delta_e}}$ more negative than the average values obtained from flight. Since it was desirable to determine the effects of each modification on the hinge moments, tests were made of modification A, then of modification B. The effects of modification C were obtained with horns 3 and 4, and these effects applied to the other horns.

The main effect of increasing the elevator gap and adding the tab-linkage cut-out (modifications A and B, respectively) was to increase considerably the negative value of $C_{h_{\delta_e}}$. Combination of modifications A and B decreased C_{h_α} by only 0.0002. The effect of altering the elevator contour (change from modification B to modification C) was to increase the value of C_{h_α} by 0.0005 and to increase the value of $C_{h_{\delta_e}}$ by 0.0008. It is very likely that the positive increase in the hinge-moment parameters was due largely to the increase in the trailing-edge angle of the elevator (modification C). (See reference 2.)

The effect of changing the horn area on the hinge-moment parameters (fig. 21) shows that the variation of C_{h_α} and $C_{h_{\delta_e}}$ for both modifications B and C is approximately a linear function of the ratio of horn area moment to elevator area moment over the range of horns tested. The point for no horn was obtained from reference 3. It must be remembered that these parameters as well as those in table II were obtained over a small elevator-deflection and angle-of-attack range and are not the average values over the flight range.

The variation of elevator hinge moments with elevator deflection for three of the horns tested is shown in figure 22. Hinge moments for the plain elevator (no horn) were obtained from reference 3.

In estimating control characteristics, the actual hinge moments and not the slopes (C_{h_α} and $C_{h_{\delta_e}}$) should be used to determine the incremental values of C_h.

Lift Characteristics

The lift parameters C_{L_α}, $C_{L_{\delta_e}}$, and α_{δ_e} were not affected appreciably by changes in the size of the horn or by the surface modifications. The effects on the parameters are shown in table II, which includes a summary of the lift parameters for the various arrangements tested. Enlarging the elevator gap (modification A) produced the greatest change; that is, both $C_{L_{\delta_e}}$ and α_{δ_e} decreased in magnitude.

Tab Characteristics

The results of the tab tests for the original tail with horn 1 are shown in figures 8 to 11, and tab tests with modification C and horn 4 are shown in figures 18 to 20. A summary of the tab results ($C_{L_{\delta_t}}$ and $C_{h_{\delta_t}}$) is included in table II.

Tab deflection caused only small variations on the elevator hinge-moment parameters C_{h_α} and $C_{h_{\delta_e}}$. The main effect was a displacement of the elevator hinge-moment curves. Note that the combined effect of surface modification and horn variation (table II) caused no noticeable effect on the value of $C_{h_{\delta_t}}$.

Estimated Airplane Characteristics and Comparison with Flight Results

Several control characteristics of the airplane were estimated for each of the configurations tested. The characteristics are tabulated in table II for an easy comparison. The control characteristics were estimated from the geometric characteristics of the airplane shown in table I and from the control-surface deflection as determined from flight tests of the airplane. The method used for the stick-force computation is given in the appendix.

Table II includes, in addition to the estimated control characteristics of the airplane, results of flight tests for a direct comparison with the tunnel data. In all cases, the values given are for a normal center-of-gravity location of 25.5 percent of the airplane mean aerodynamic chord.

The stick forces from flight tests show excellent agreement with the estimated stick forces for the model with modification C and horn 1. This close agreement of the modified model emphasizes the importance of simulating airplane surface irregularities on models if any reasonable comparison with flight tests is sought.

The flight tests and the tunnel tests for the original elevator show that the airplane had undesirable control characteristics, that is, high stick forces in maneuvers and in trim changes due to flap. The tail showing the most promise from wind-tunnel tests, modification C and horn 3, which incorporated a balancing tab in place of the trim tab, was flight tested. Results of the flight tests (table II) indicate, as is also indicated from wind-tunnel tests, that this arrangement decreased considerably the undesirably large control forces and generally made these forces acceptable to the flying requirements (reference 4) for this type airplane. There was close agreement between wind-tunnel data and flight data for the airplane with the revised tail.

A comparison between flight and estimated characteristics for the airplane with modification C and horn 3 is shown in figure 23. The stick-force variation with airspeed is very similar in the power-off condition for both instances. The power-on condition showed a larger discrepancy, mainly a trim change. This trim change is probably due to the fact that variables caused by power could not be adequately accounted for in the calculations.

CONCLUSIONS

A wind-tunnel investigation was conducted to determine the effect of unshielded horn balances on the aerodynamic characteristics of a 0.5-scale model of the left horizontal tail surface of a torpedo bomber. Control characteristics for the airplane were estimated from the wind-tunnel data and compared with flight data. The following conclusions were indicated:

1. The variation of hinge-moment coefficient with angle of attack and with elevator deflection caused by a change in the size of the unshielded horn was approximately a linear function of the ratio of horn area moment to elevator area moment.

2. The lift parameters were not affected appreciably by changes in the size of the horn or by the surface modifications introduced.

3. Very close agreement between the control-force characteristics of the airplane as determined from flight data and characteristics estimated from wind-tunnel data was obtained when the airplane surface irregularities were simulated on the model.

Langley Memorial Aeronautical Laboratory
National Advisory Committee for Aeronautics
Langley Field, Va., April 25, 1947

APPENDIX

COMPUTATION OF STICK FORCES

All the stick forces except the values of dF_s/dn were computed from the relationship

$$F_s = \frac{1175}{C_L} \Delta C_h$$

which was derived from the elevator dimensions and the geometric characteristics of the airplane given in table I. For these computations the elevator-stick deflection curve was assumed to be a straight line. The values of ΔC_h were obtained from the hinge-moment curves using the deflections of elevator and angles of attack determined from the flight-test results. The angle of attack was determined from the flight data by subtracting the force due to elevator deflection from the total force and determining the angle of attack from the flight value of C_{h_α}. For the computations of trim characteristics the value of q at the tail was assumed to be the free-stream value of q. This assumption was made since the tail is located well above the thrust axis, and it is believed that there should be less than 10-percent change in q due to application of power.

The estimated values of dF_s/dn were obtained from the relationship

$$\frac{dF_s}{dn} = \left(12 \frac{0.69}{\alpha_{\delta_e}} \frac{C_{h_{\delta_e}}}{-0.0015} + 28 \frac{C_{h_\alpha}}{0.0030} \right) \frac{\Delta C_{h_{curves}}}{\Delta C_{h_{slopes}}}$$

This method depends upon determining the increment of stick force caused by elevator deflection δ_e and the increment of stick force caused by angle of attack α from flight-test data. For these calculations the flight-test data for horn 1 were used. The stick forces for any of the other elevator configurations were obtained by first multiplying the increment of stick force due to δ_e by the reciprocal of the lift-effectiveness ratio and hinge-moment-

coefficient ratio and then multiplying the stick force due to α by the hinge-moment-coefficient ratio. The multiplication factor $\frac{\Delta C_{h_{curves}}}{\Delta C_{h_{slopes}}}$ corrects for the nonlinearity of the hinge-moment curves.

REFERENCES

1. Swanson, Robert S., and Toll, Thomas A.: Jet-Boundary Corrections for Reflection-Plane Models in Rectangular Wind Tunnels. NACA Rep. No. 770, 1943.

2. Jones, Robert T., and Ames, Milton B., Jr.: Wind-Tunnel Investigation of Control-Surface Characteristics. V - The Use of a Beveled Trailing Edge to Reduce the Hinge Moment of a Control Surface. NACA ARR, March 1942.

3. Liddell, Robert B., and Lockwood, Vernard E.: Wind-Tunnel Investigation of Rounded Horns and of Guards on a Horizontal Tail Surface. NACA ARR No. L4J16, 1944.

4. Gilruth, R. R.: Requirements for Satisfactory Flying Qualities of Airplanes. NACA Rep. No. 755, 1943.

TABLE I

GEOMETRIC CHARACTERISTICS OF AIRPLANE AND 0.5-SCALE SEMISPAN MODEL OF HORIZONTAL TAIL SURFACE

[Center-of-gravity location, 25.5 percent M.A.C.]

Geometric characteristics	Airplane	Model
Gross weight, lb	12,910	-----
Wing area, ft^2	490	-----
Stick length, ft	1.5	-----
Total stick travel, deg	55	-----
Elevator movement relative to stabilizer, deg		
Up	17.7	-----
Down	11	-----
Horizontal-tail area, sq ft	111.5	13.69
Horizontal-tail span, ft	20.83	5.204
Elevator area behind hinge line, sq ft	48	5.93
Elevator root-mean-square chord, ft	2.536	1.268
Slope of airplane lift curve	0.078	-----
$\partial\epsilon/\partial\alpha$	0.5	-----

NATIONAL ADVISORY
COMMITTEE FOR AERONAUTICS

TABLE II

CONTROL PARAMETERS AND STICK FORCES FOR VARIOUS ARRANGEMENTS OF HORIZONTAL TAIL SURFACE

Elevator modification	Horn	C_{L_α}	$C_{L_{\delta_e}}$	$C_{L_{\delta_t}}$	α_{ϵ_e}	C_{h_α} (a)	$C_{h_{\delta_e}}$ (a)	$C_{h_{\delta_t}}$ (a)	Elevator deflection required to land (deg)	Stick force required to land (lb) (b)	$\frac{dF_s}{dn}$ (lb) (c)	Stick force required to trim flaps (lb) (d)
Wind-tunnel tests												
Original	1	0.059	0.043	0.003	-0.72	0.0018	-0.0025	-0.0029	-17	39	34	-30
A	1	.059	.041	-----	-.70	.0019	-.0030	-------	-17	41	39	-32
B	1	.059	.041	-----	-.70	.0016	-.0035	-------	-17	40	42	-30
[e]C	1	.058	.040	-----	-.69	.0021	-.0027	-------	-17	40	40	-40
B	2	.058	.042	-----	-.70	.0009	-.0040	-------	-17	40	39	-22
B	3	.058	.042	-----	-.69	-.0001	-.0050	-------	-17	40	37	-7
[f]B	3	.058	.041	.003	-.69	-.0001	-.0035	[g]-.0029	-17	22	27	-4
C	3	.057	.041	-----	-.68	.0004	-.0042	-------	-17	38	31	-13
[f]C	3	.057	.040	.003	-.68	.0004	-.0027	[g]-.0030	-17	20	21	-10
B	4	.057	.041	-----	-.70	-.0009	-.0057	-------	-17	40	27	-2
C	4	.057	.040	.003	-.69	-.0004	-.0050	-.0030	-17	40	24	-4
Flight tests												
C	1	-----	-----	-----	-----	[h]0.0030	[h]-0.0015	-------	-17	--	40	-42
C	3	-----	-----	-----	-----	-------	--------	-------	---	--	26	-12

[a] Parameters of C_h for wind-tunnel tests are for $\delta_e = 0°$, $\delta_t = 0°$, and $\alpha = 0°$.

[b] V_i = 76 mph; trimmed at 120 mph with flaps down.

[c] V_i = 217 mph; average for 2.4 n; initial condition: $\delta_e = 0.5°$, $\alpha = -1°$.

[d] V_i = 120 mph; initial condition: $\delta_e = 0°$, $\alpha = 3.2°$.

[e] Estimated from effect of modification C on horns 3 and 4.

[f] $\frac{\delta_t}{\delta_e} = -0.5$; parameters include effect of tab.

[g] Estimated from similar data on other arrangements.

[h] Average value over flight range.

NATIONAL ADVISORY
COMMITTEE FOR AERONAUTICS

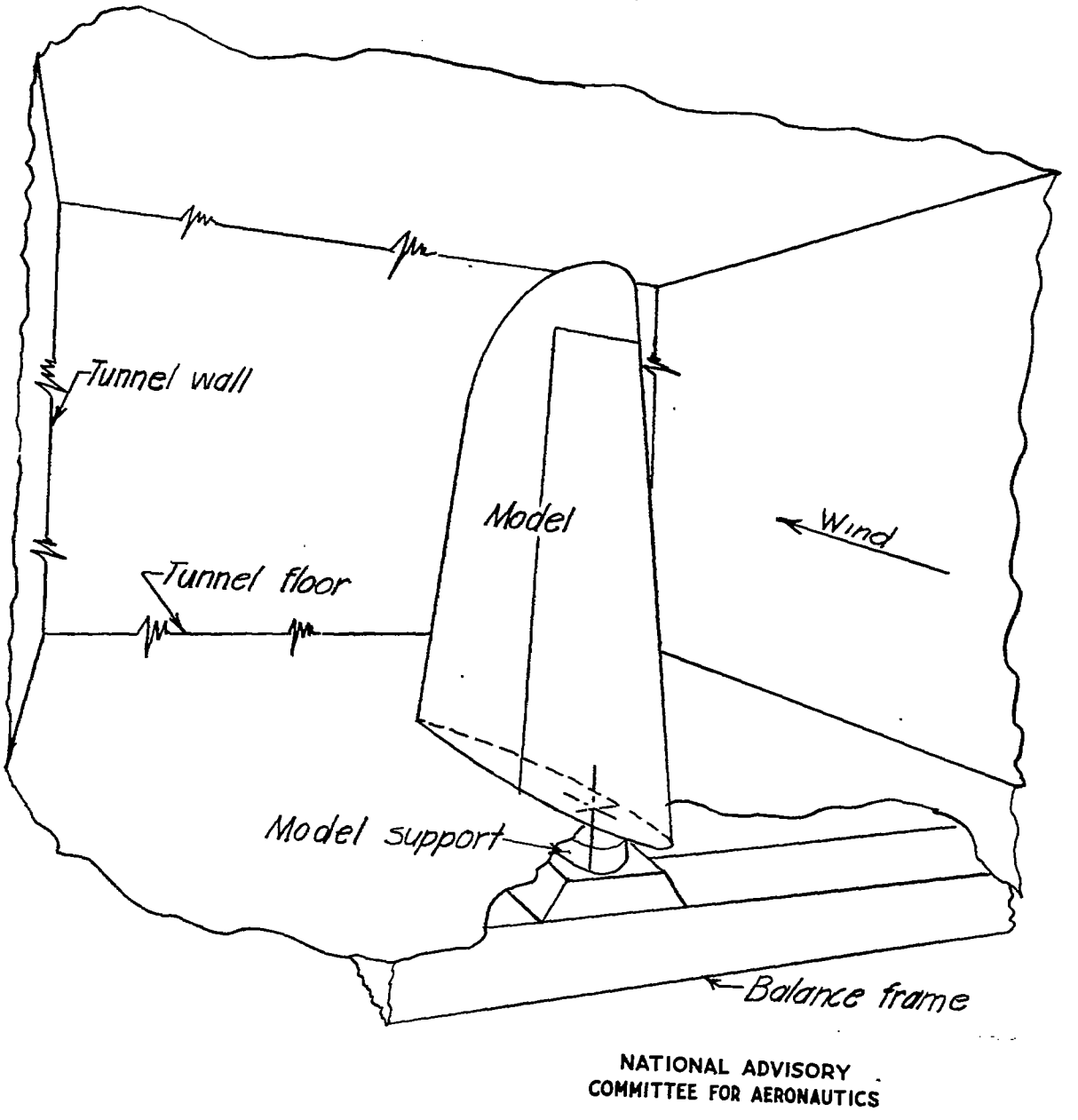

Figure 1.- Schematic diagram of test installation.

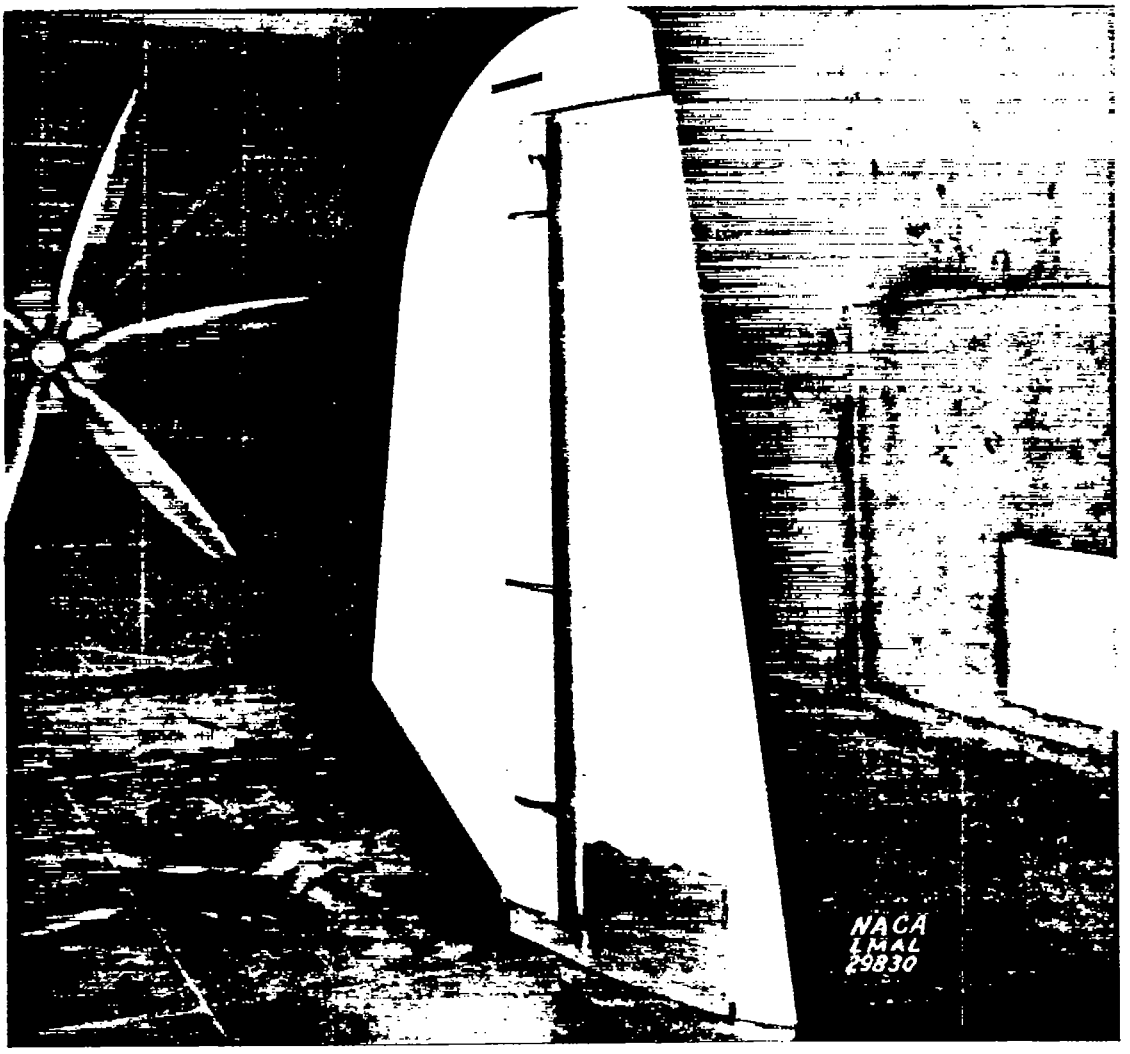

Figure 2.- Three-quarter front view of 0.5-scale semispan model of horizontal tail tested.

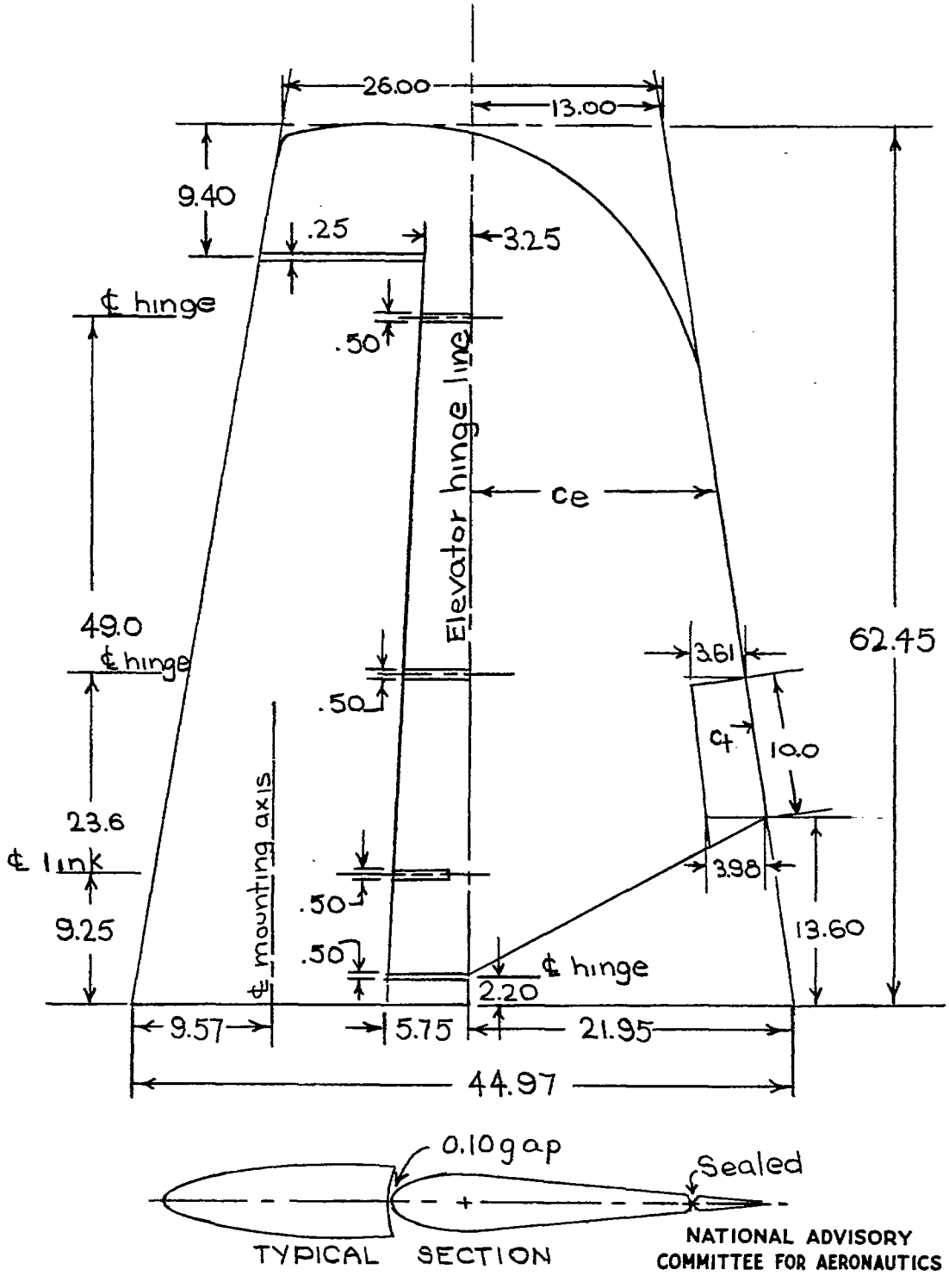

Figure 3.- Original 0.5-scale model of left horizontal tail surface. (All dimensions are in inches.)

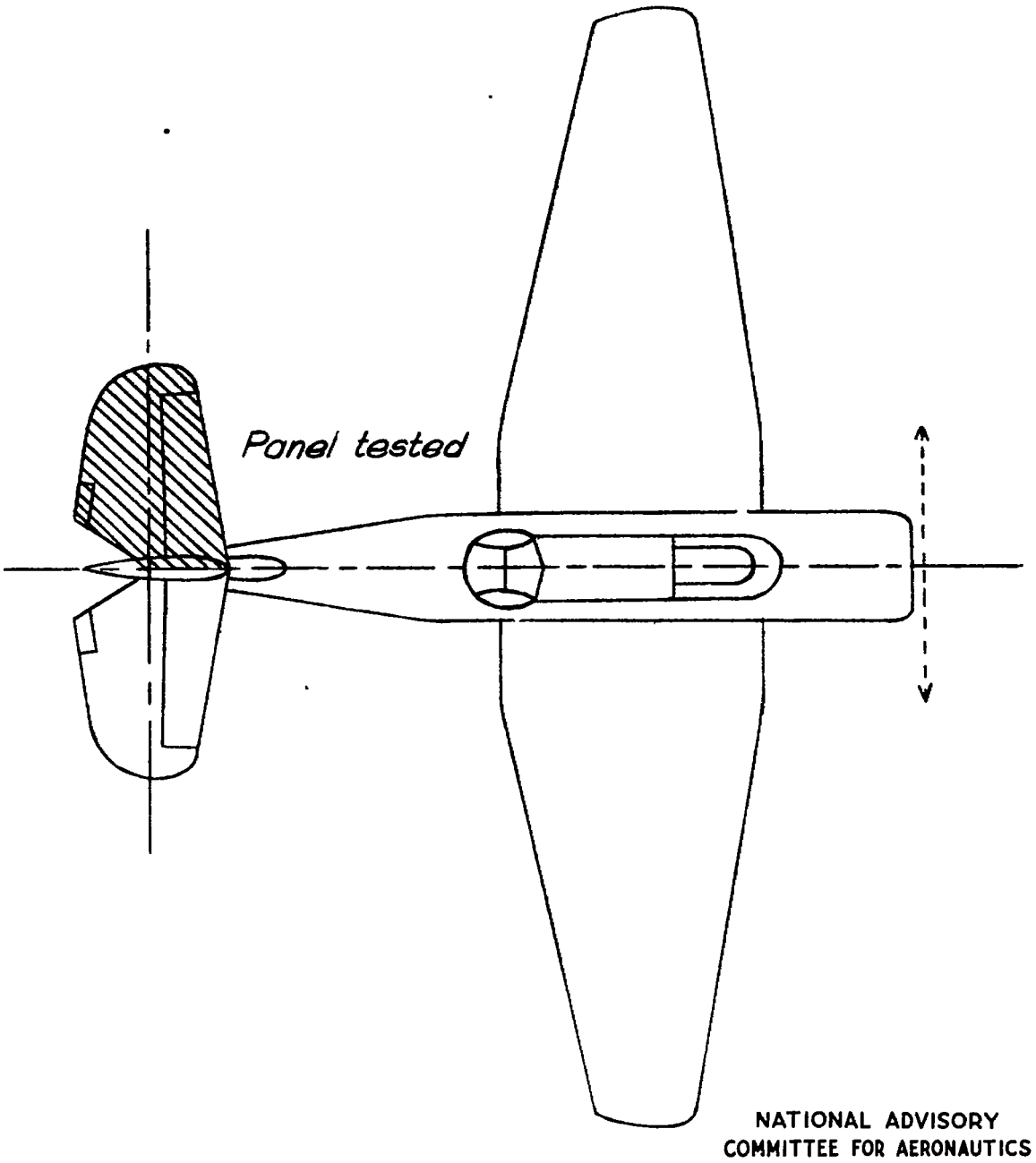

Figure 4.- Plan form of airplane.

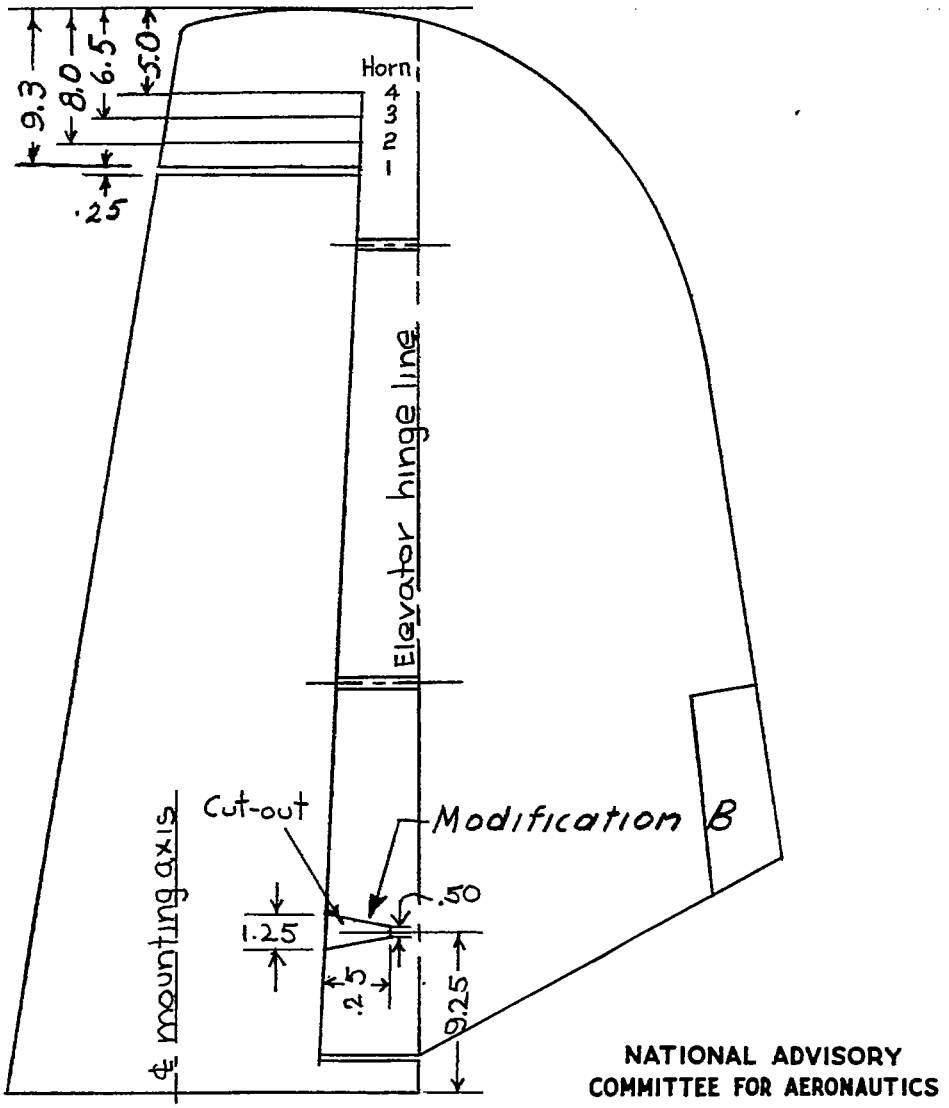

Figure 5.- Details of modifications A and B and horns 1 to 4. Modification B includes modification A. (All dimensions are in inches.)

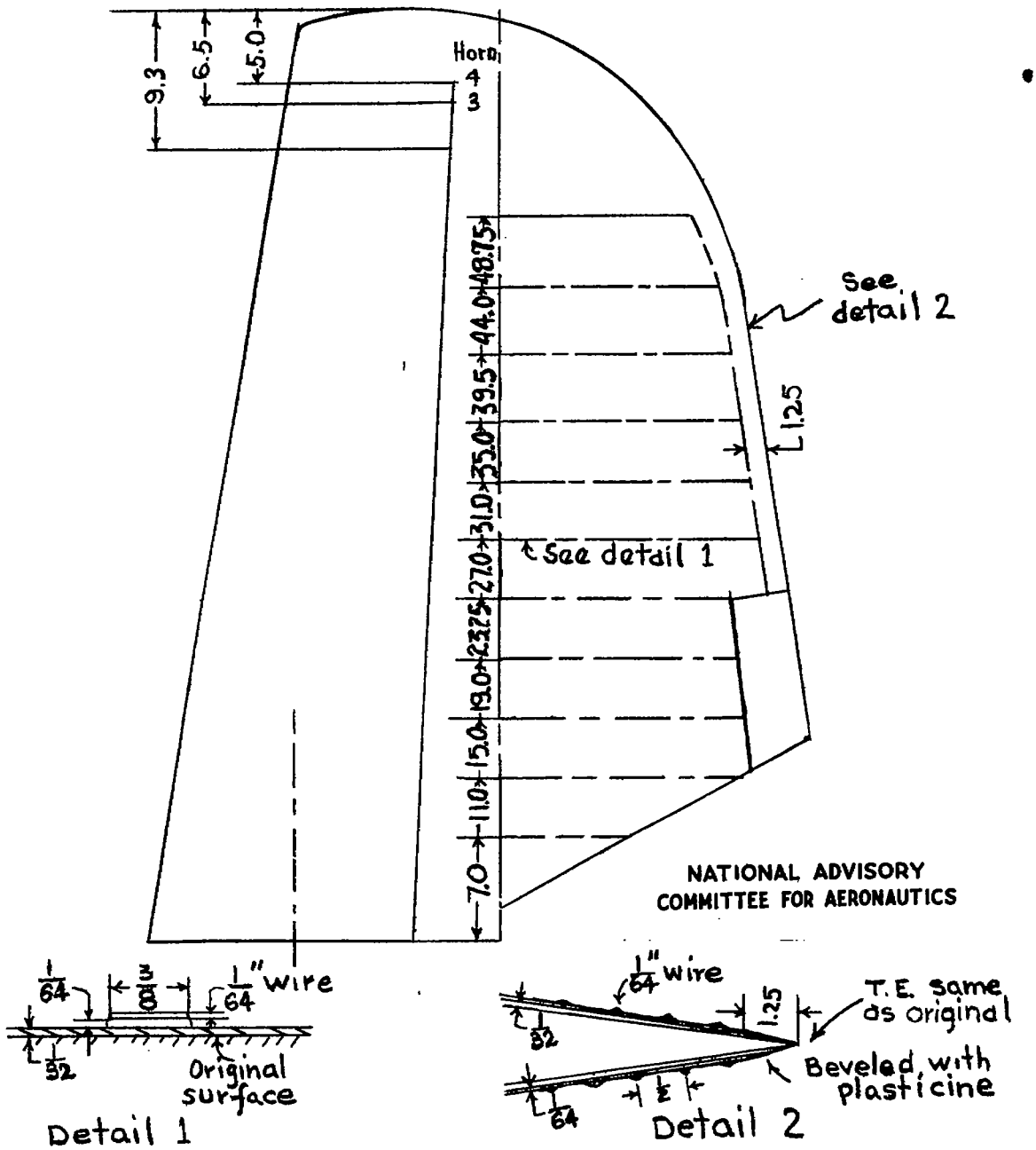

Figure 6.- Details of modification C. Modification C includes modifications A and B. (All dimensions are in inches.)

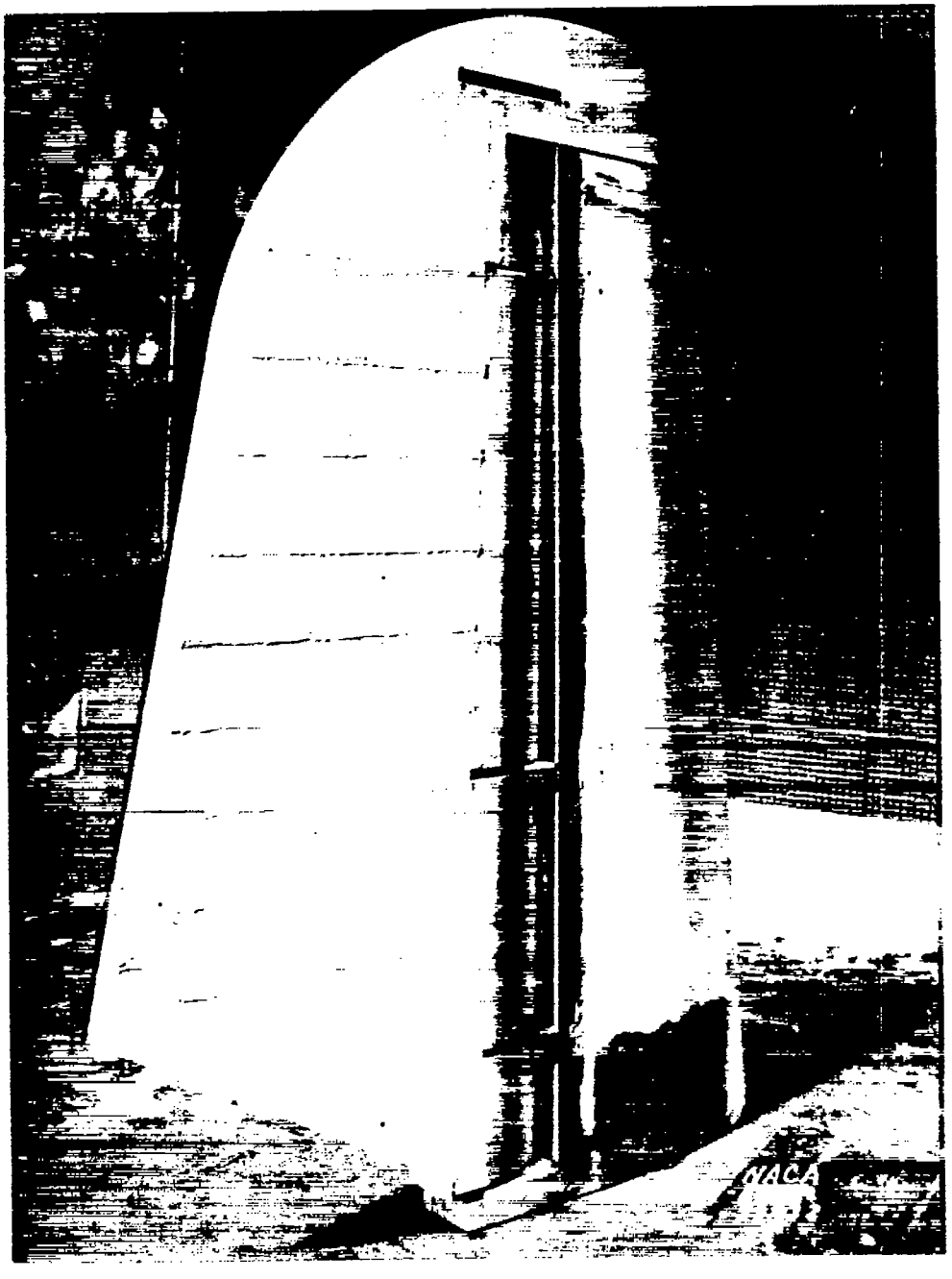

Figure 7.- Three-quarter rear view of 0.5-scale semispan model of horizontal tail tested. Modification C; horn 3.

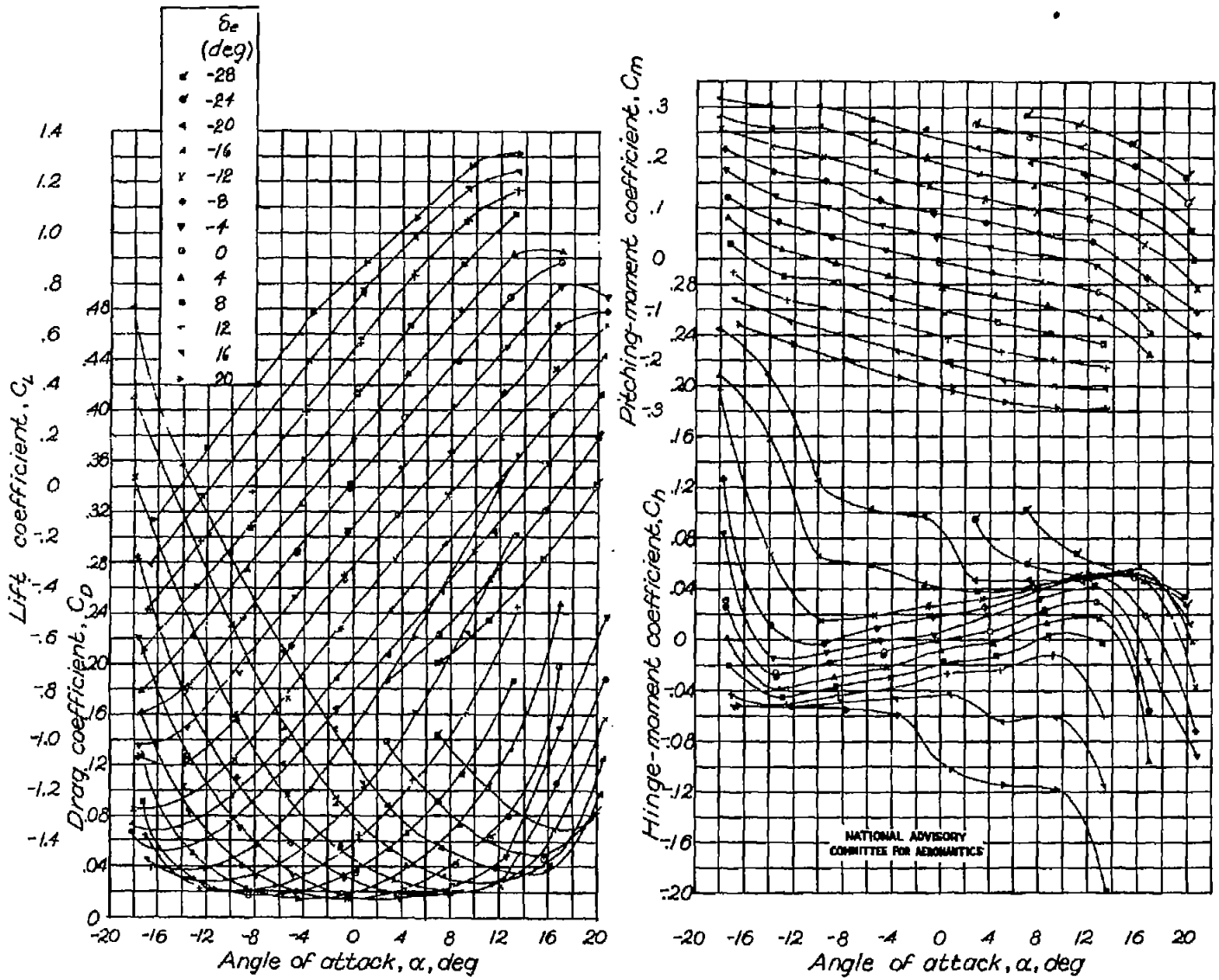

Figure 8.- Aerodynamic characterictics of the 0.5-scale model of left horizontal tail surface. Original tail; horn 1; $\delta_t = 0^\circ$.

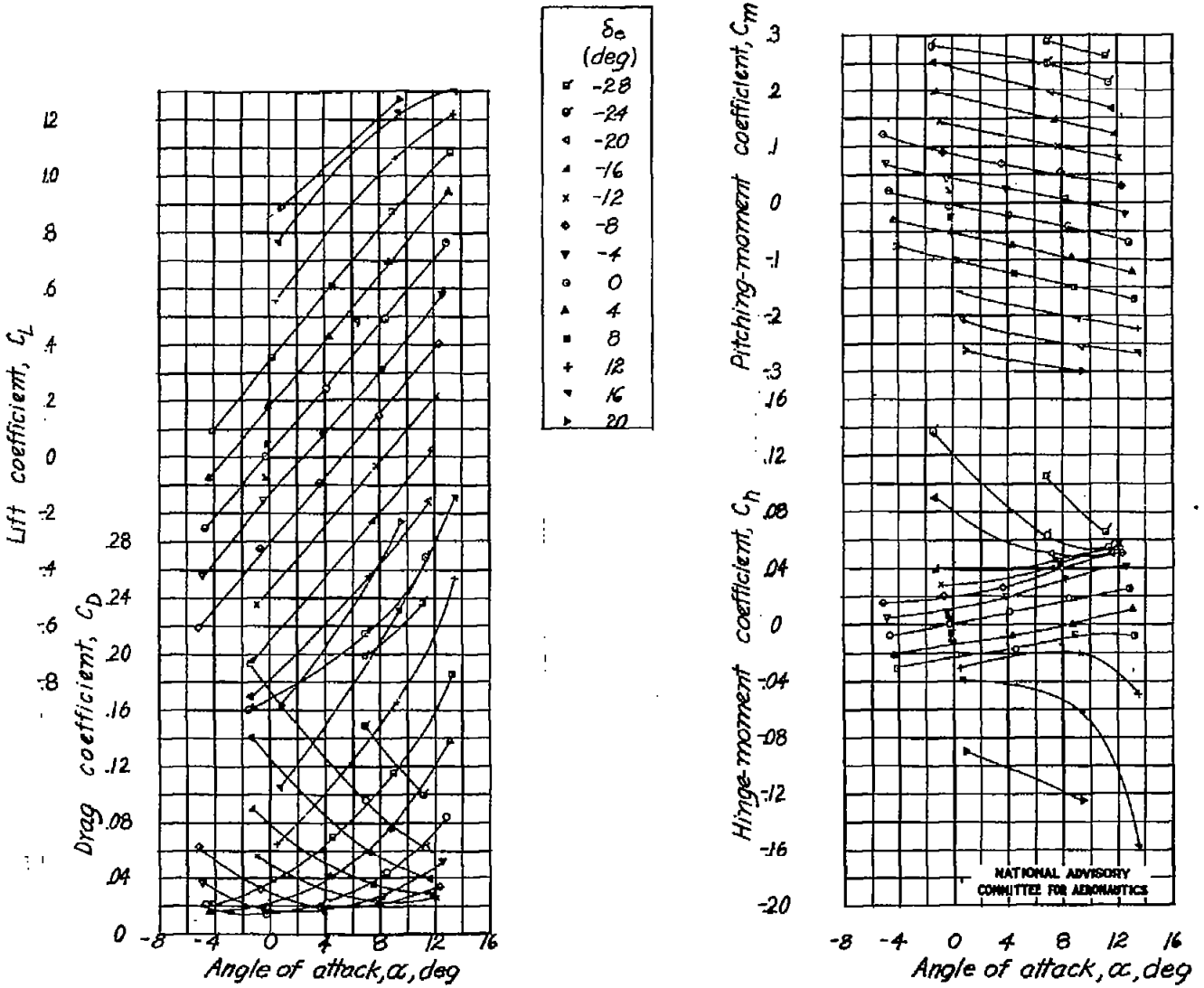

Figure 9.- Aerodynamic characteristics of the 0.5-scale model of left horizontal tail surface. Modification A; horn 1; $\delta_t = 0^\circ$.

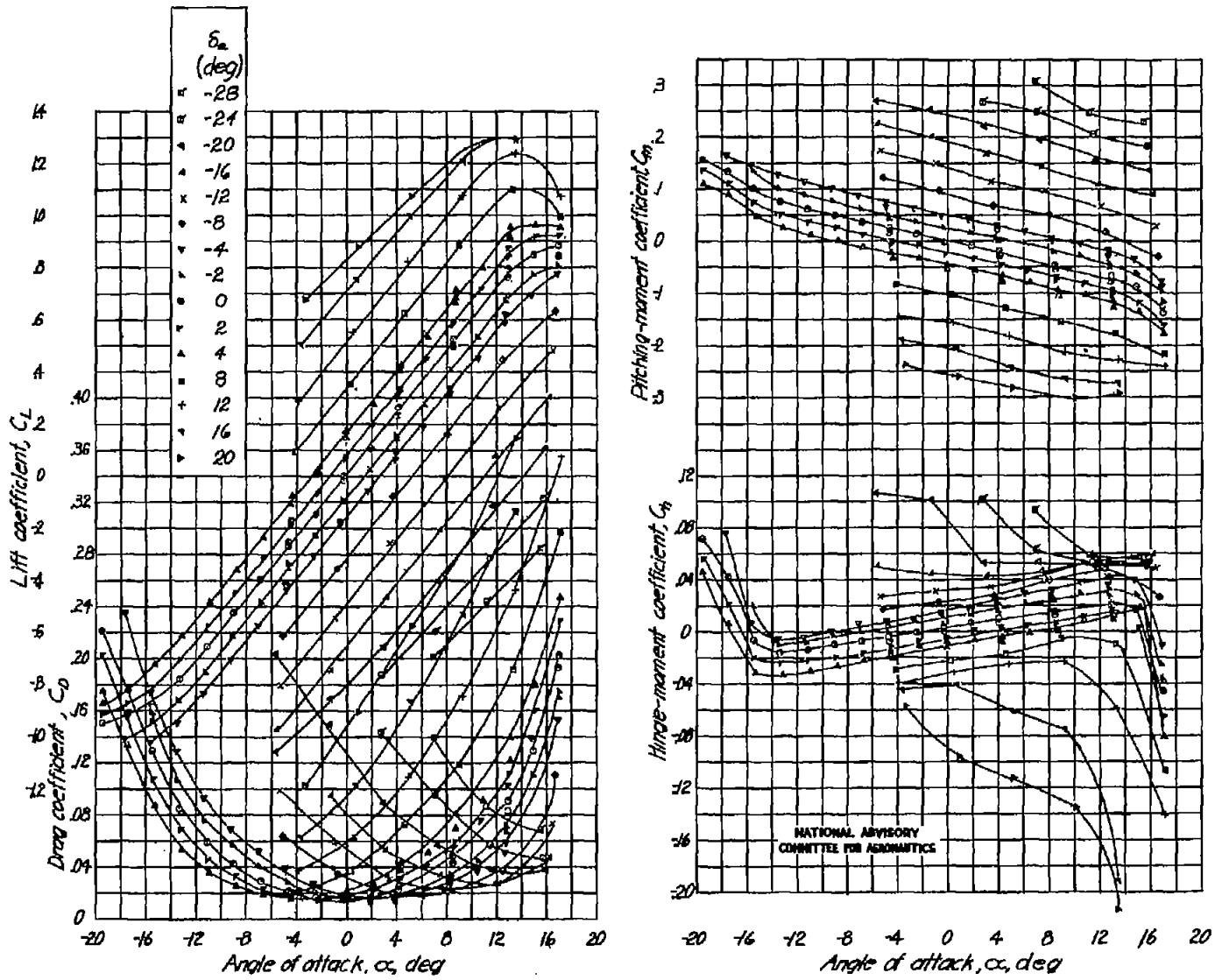

Figure 10.- Aerodynamic characteristics of the 0.5-scale model of left horizontal tail surface. Modification B; horn 1; $\delta_t = 0^\circ$.

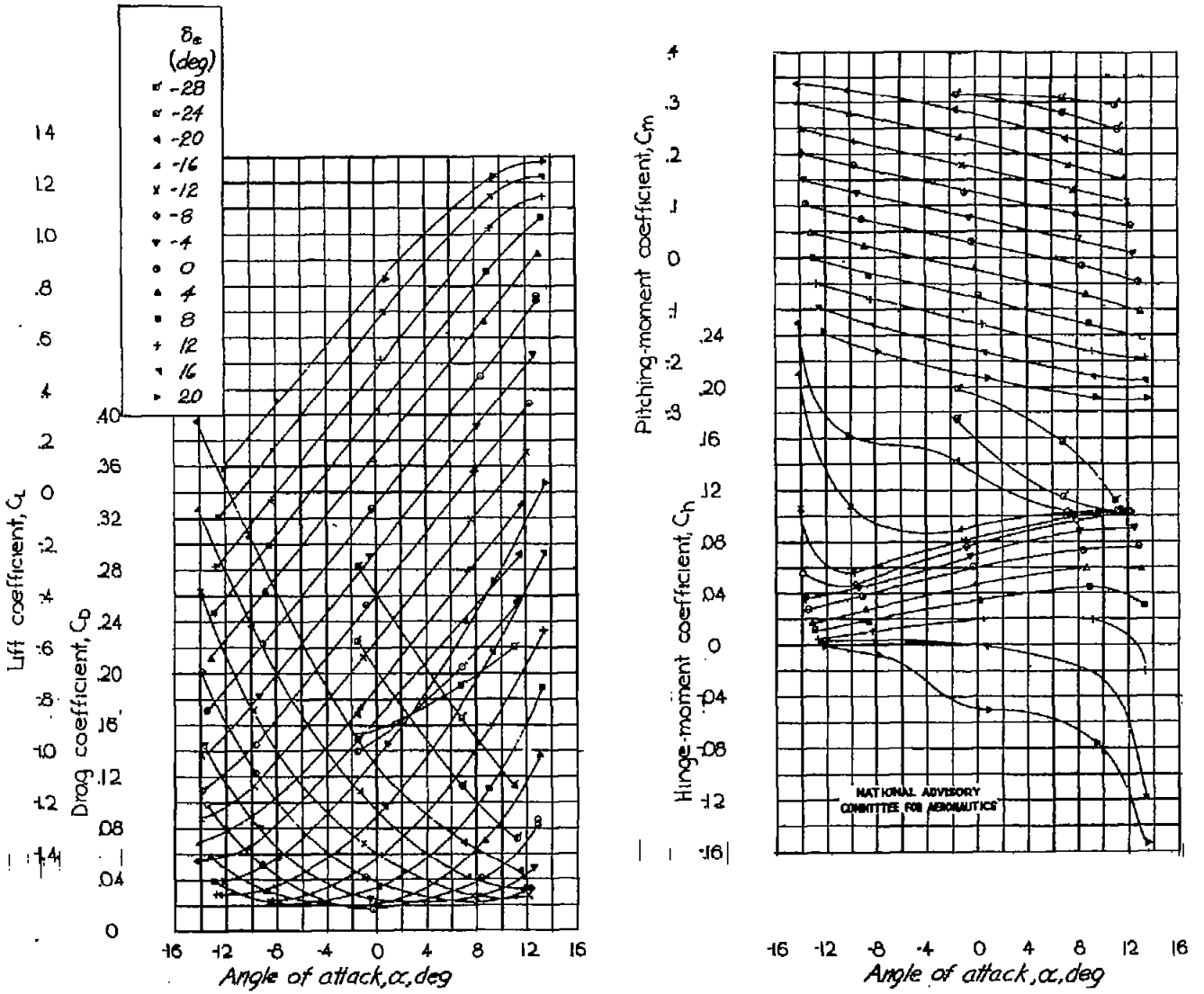

Figure 11.- Aerodynamic characteristics of the 0.5-scale model of left horizontal tail surface. Original tail; horn 1; $\delta_t = -20^\circ$.

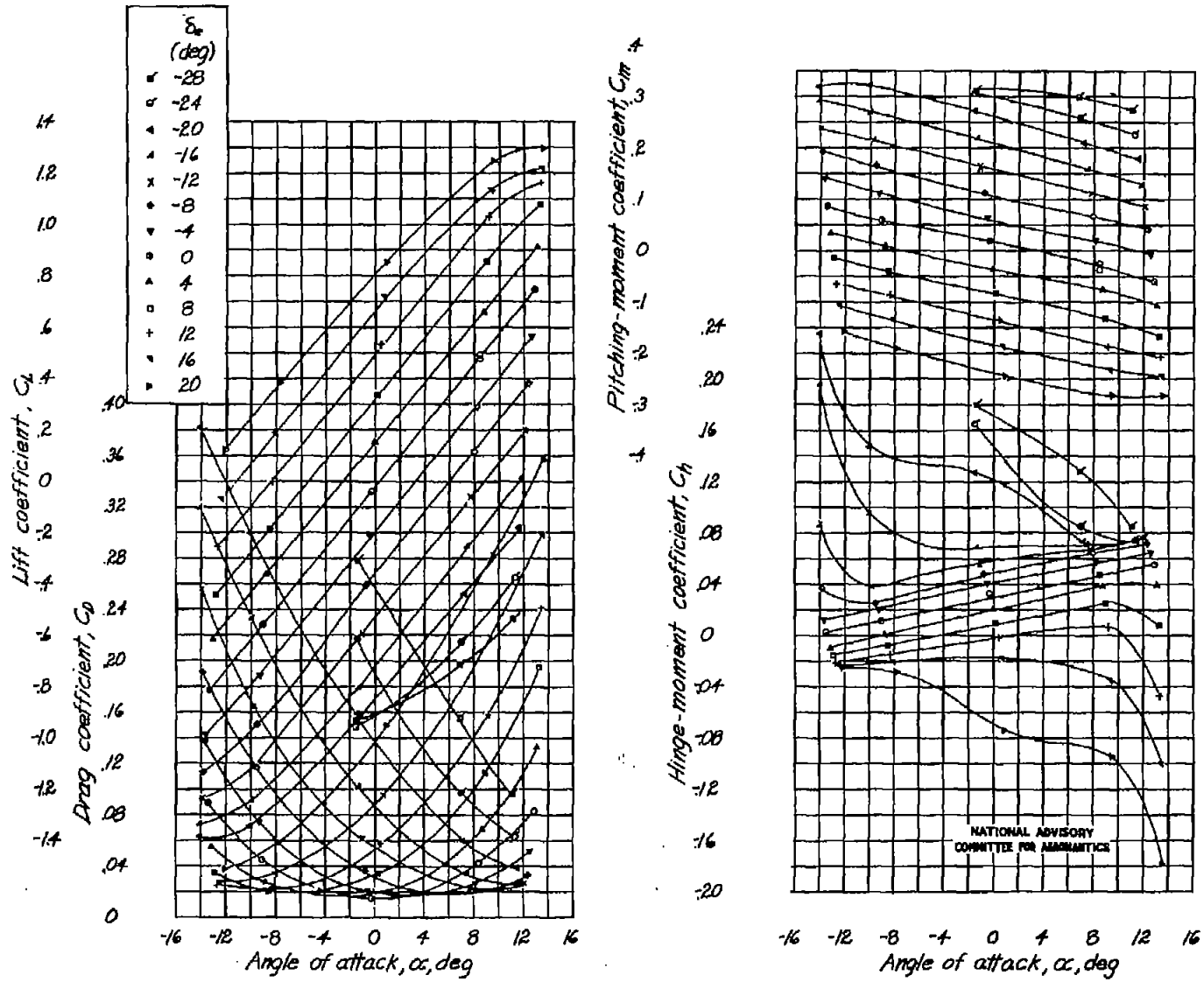

Figure 12.- Aerodynamic characteristics of the 0.5-scale model of left horizontal tail surface. Original tail; horn 1; $\delta_t = -10^\circ$.

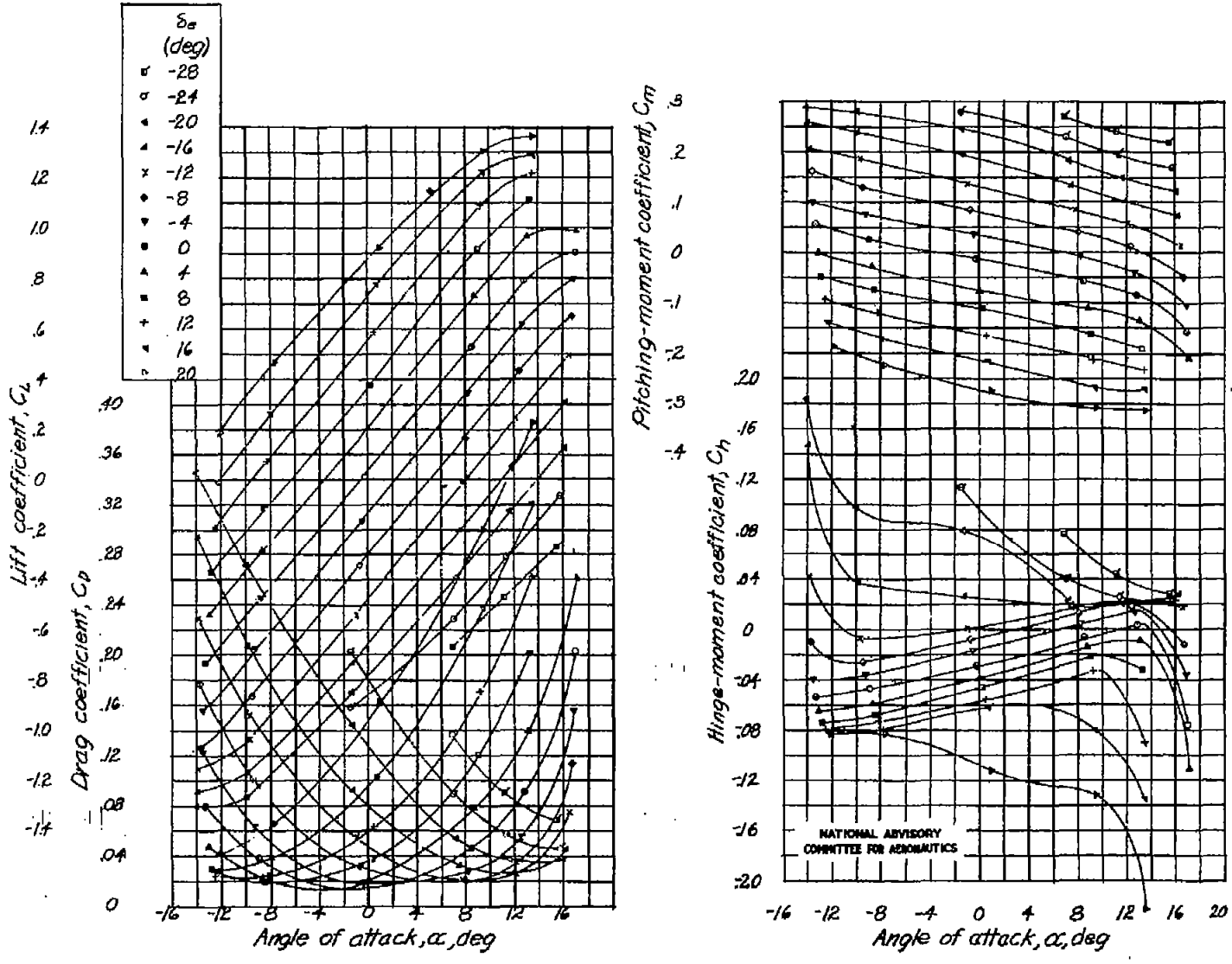

Figure 13.- Aerodynamic characteristics of the 0.5-scale model of left horizontal tail surface. Original tail; horn 1; $\delta_t = 10^o$.

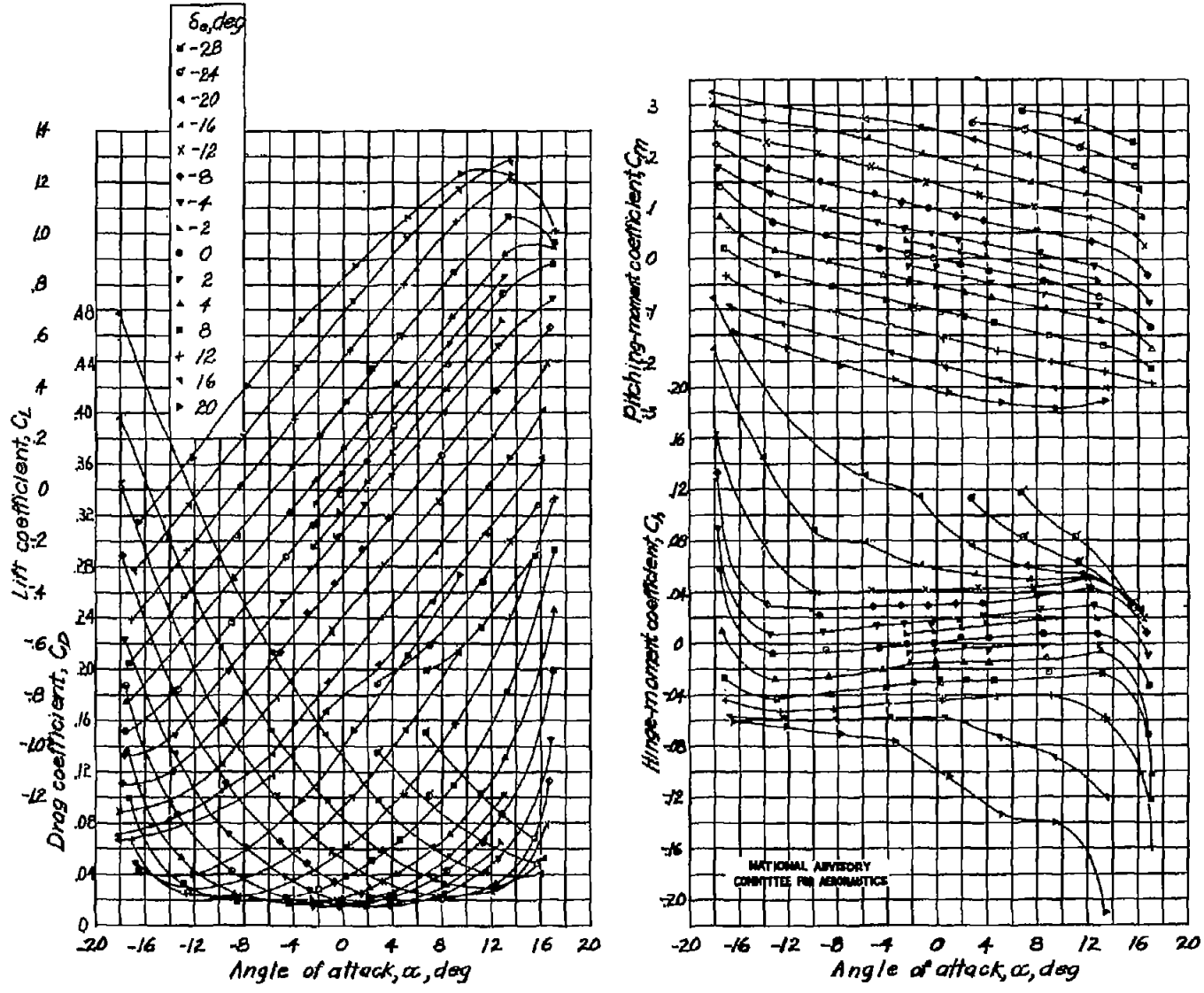

Figure 14.- Aerodynamic characteristics of the 0.5-scale model of left horizontal tail surface. Modification B; horn 2; $\delta_t = 0^\circ$.

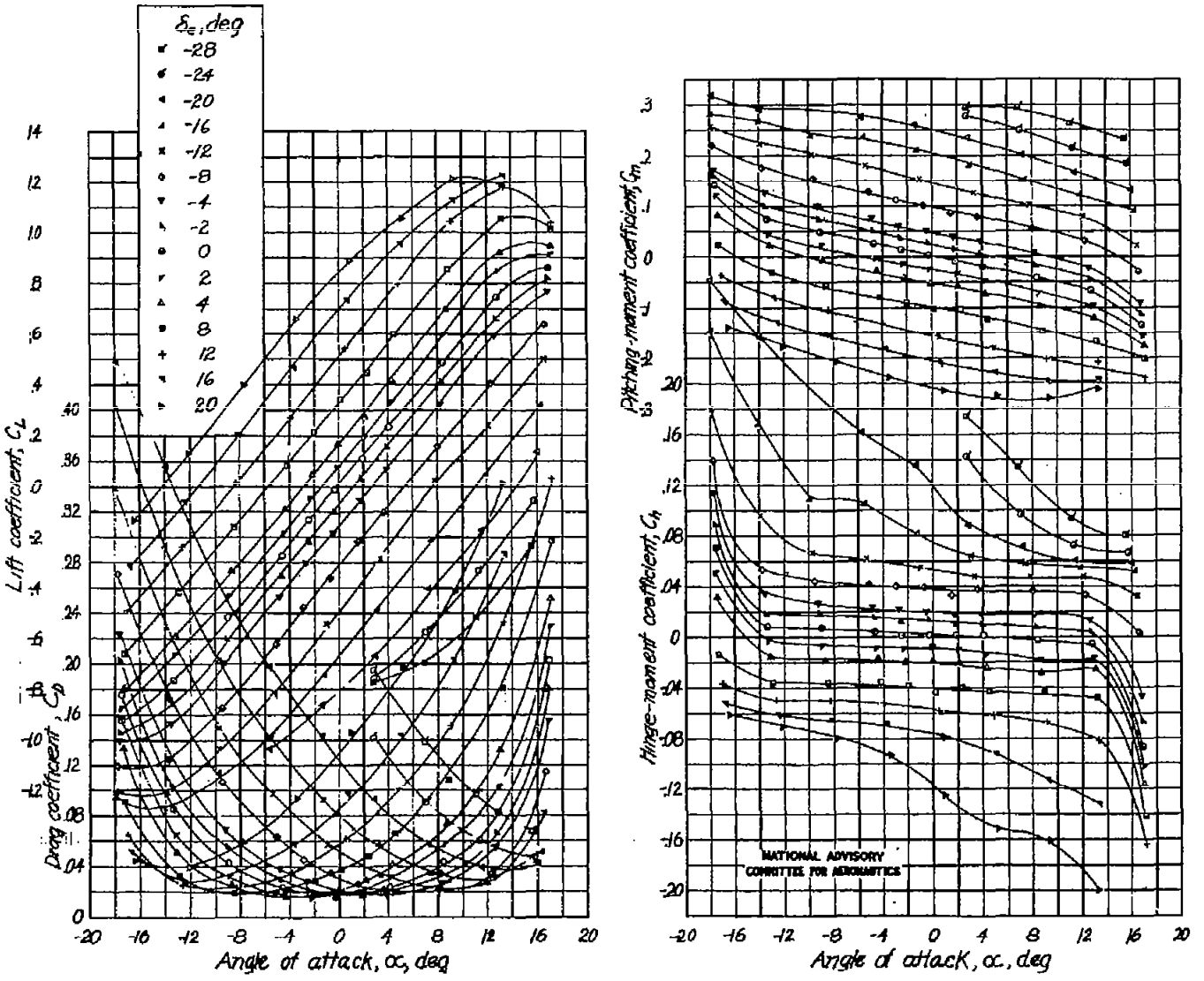

Figure 15.- Aerodynamic characteristics of the 0.5-scale model of left horizontal tail surface. Modification B; horn 3; $\delta_t = 0^\circ$.

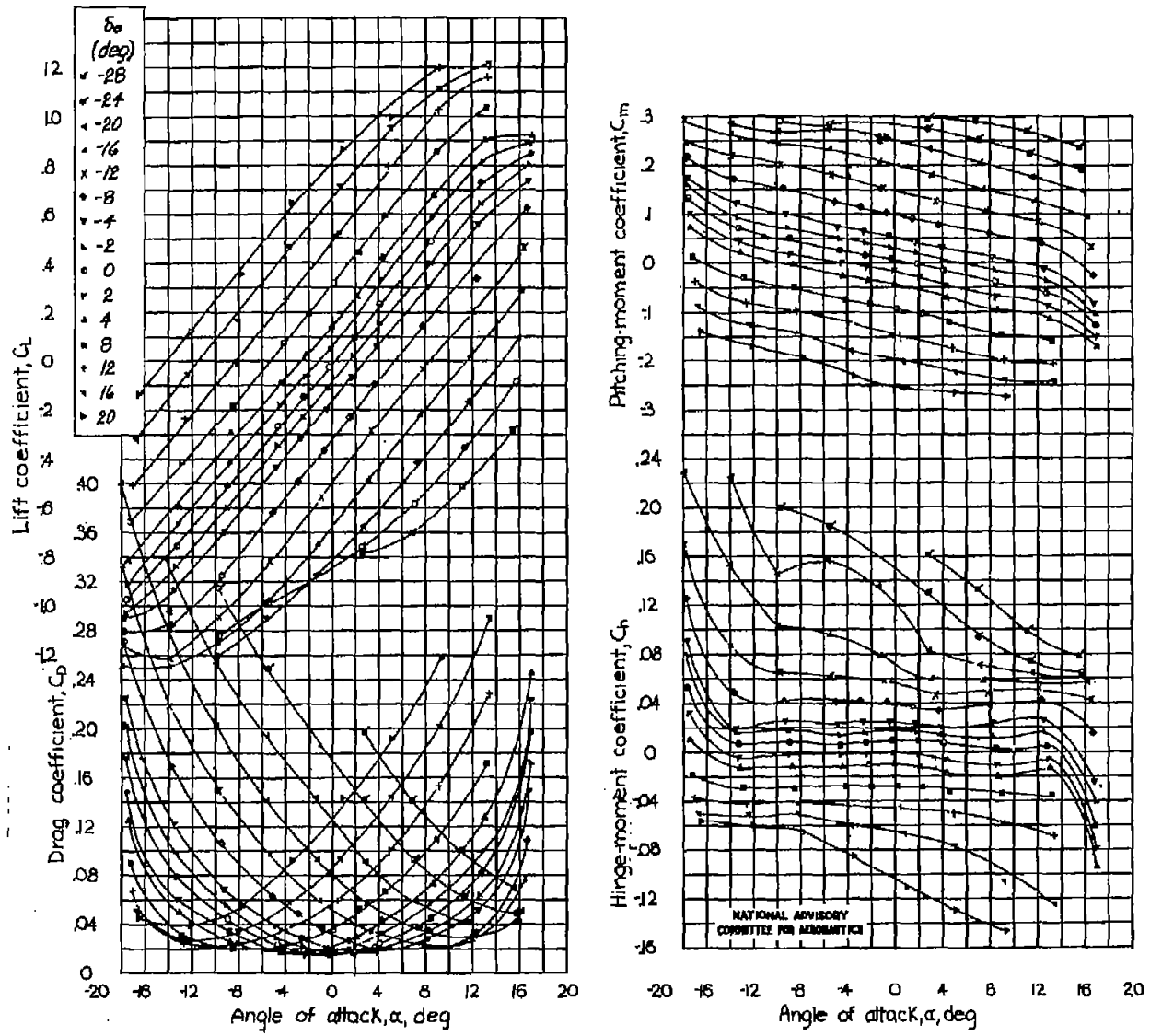

Figure 16.- Aerodynamic characteristics of the 0.5-scale model of left horizontal tail surface. Modification C; horn 3; $\delta_t = 0^\circ$.

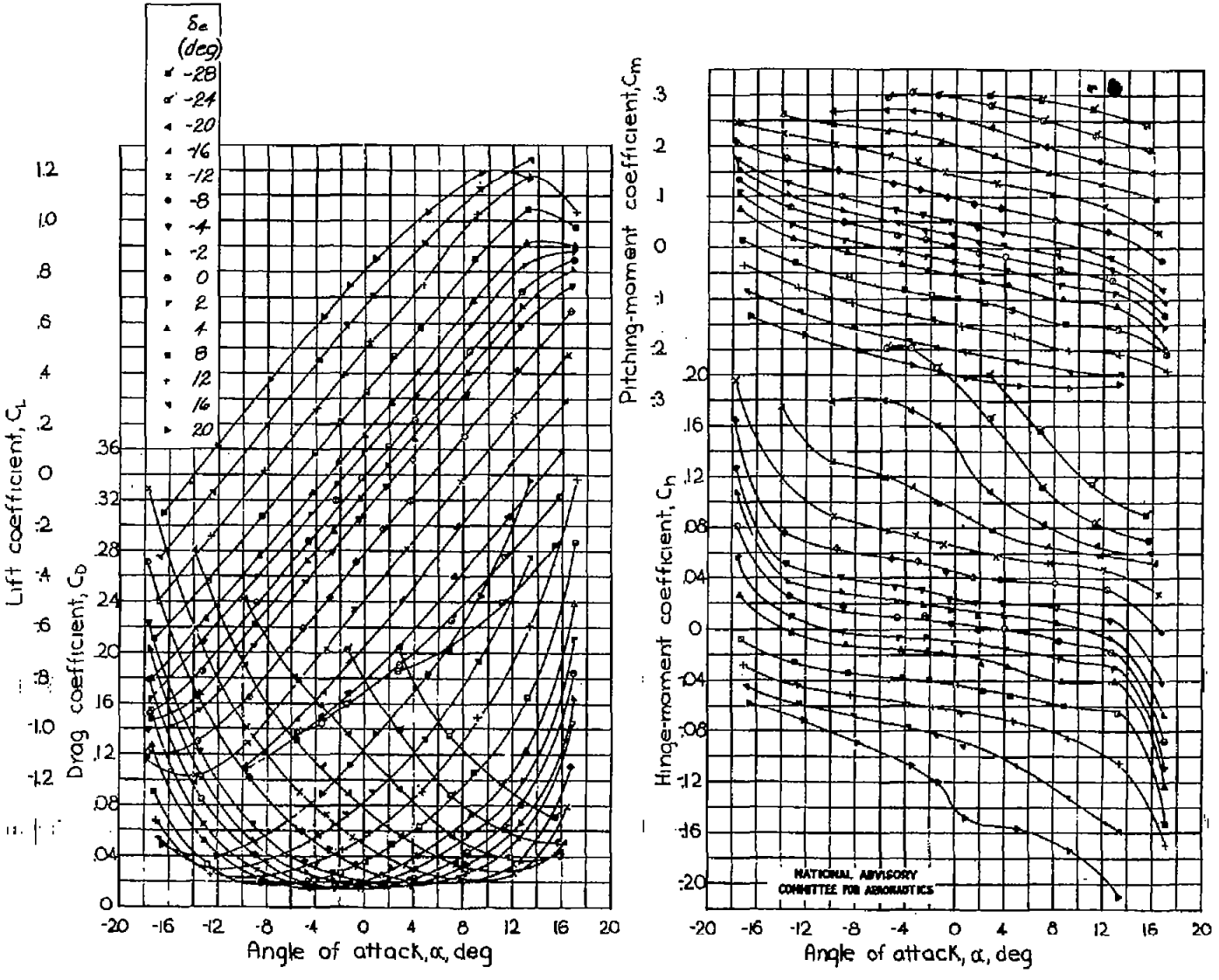

Figure 17.- Aerodynamic characteristics of the 0.5-scale model of left horizontal tail surface. Modification B; horn 4; $\delta_t = 0^\circ$.

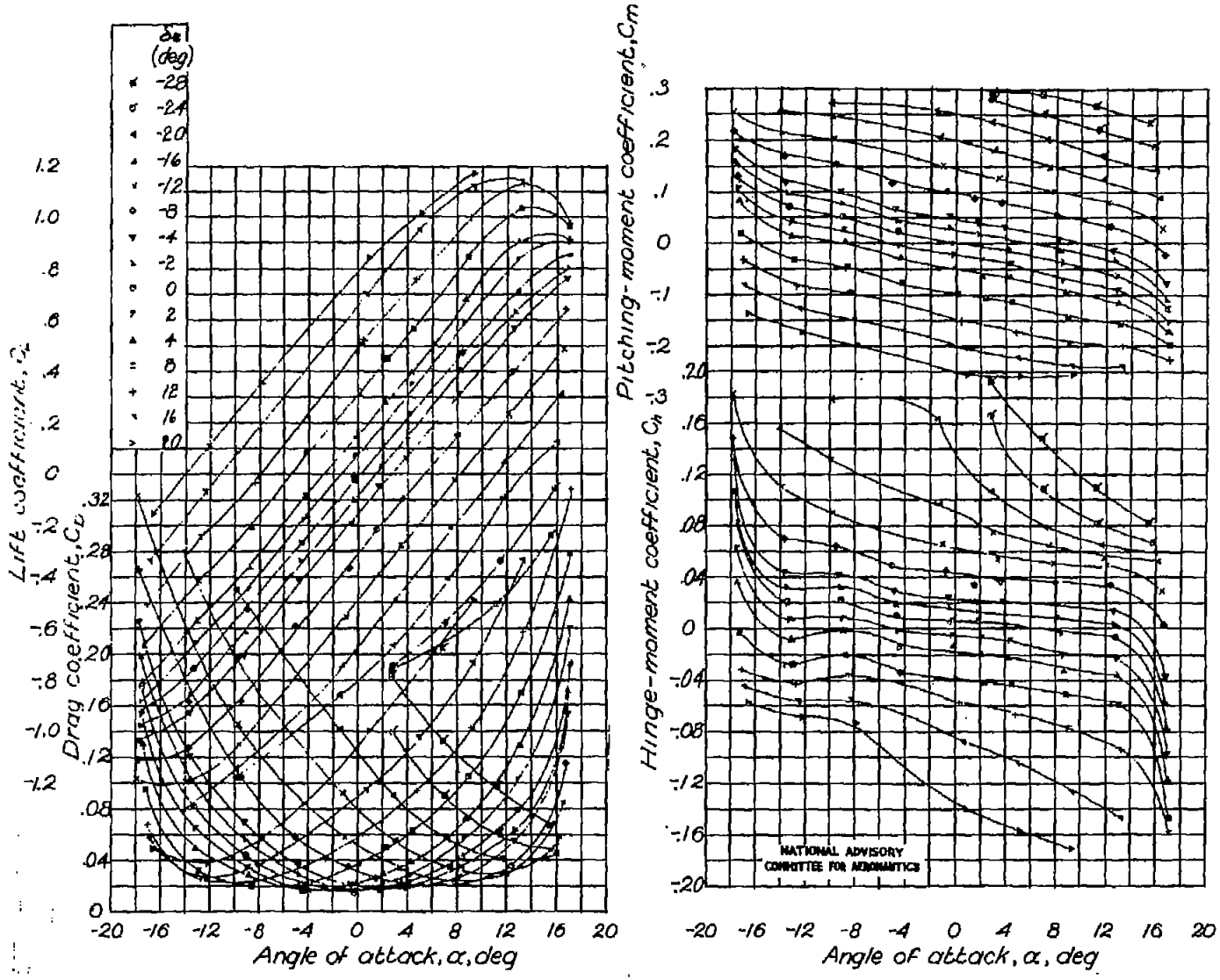

Figure 18.- Aerodynamic characteristics of the 0.5-scale model of left horizontal tail surface. Modification C; horn 4; $\delta_t = 0^\circ$.

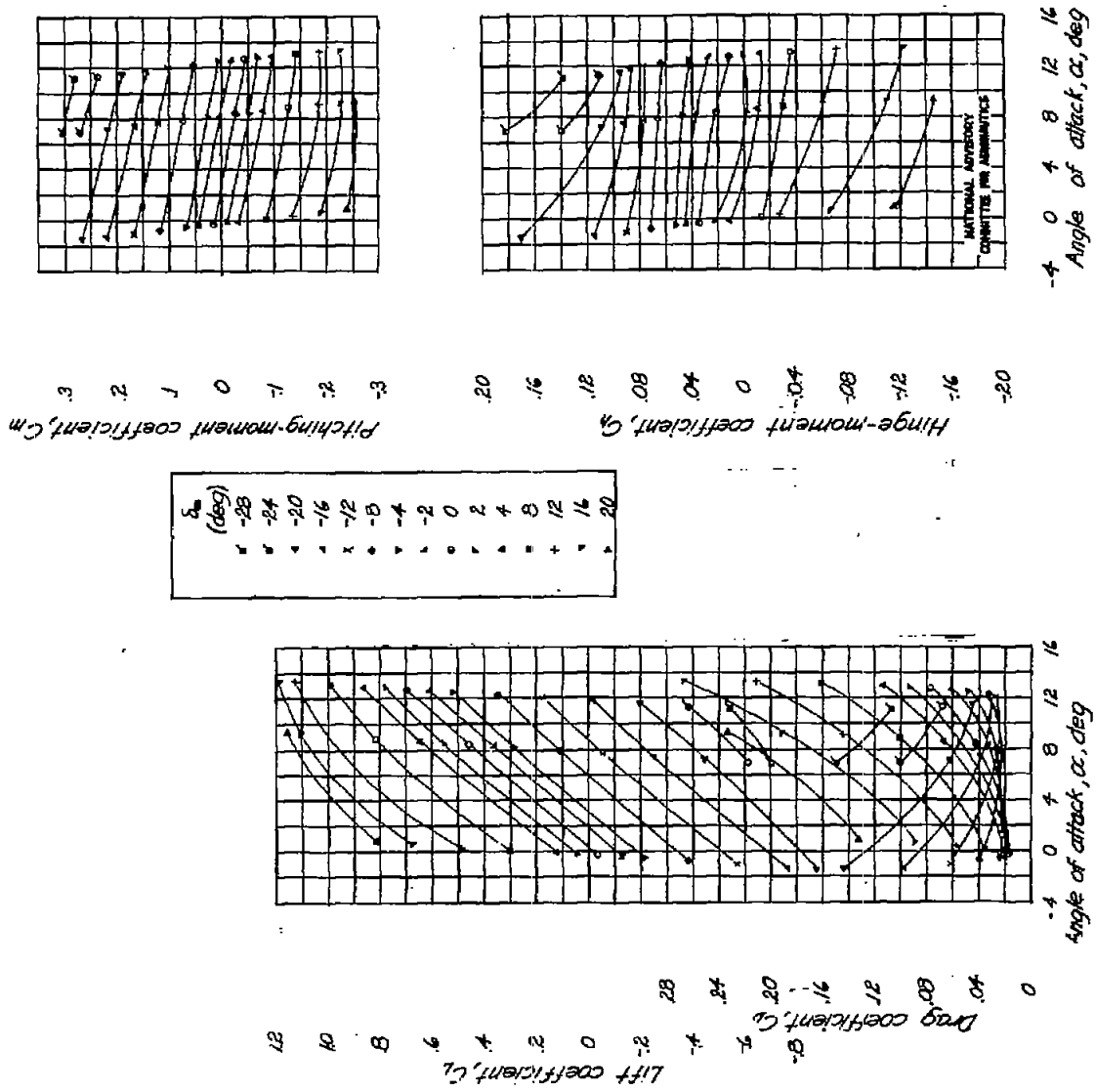

Figure 19.- Aerodynamic characteristics of the 0.5-scale model of left horizontal tail surface. Modification C; horn 4; $\delta_t = -10^\circ$.

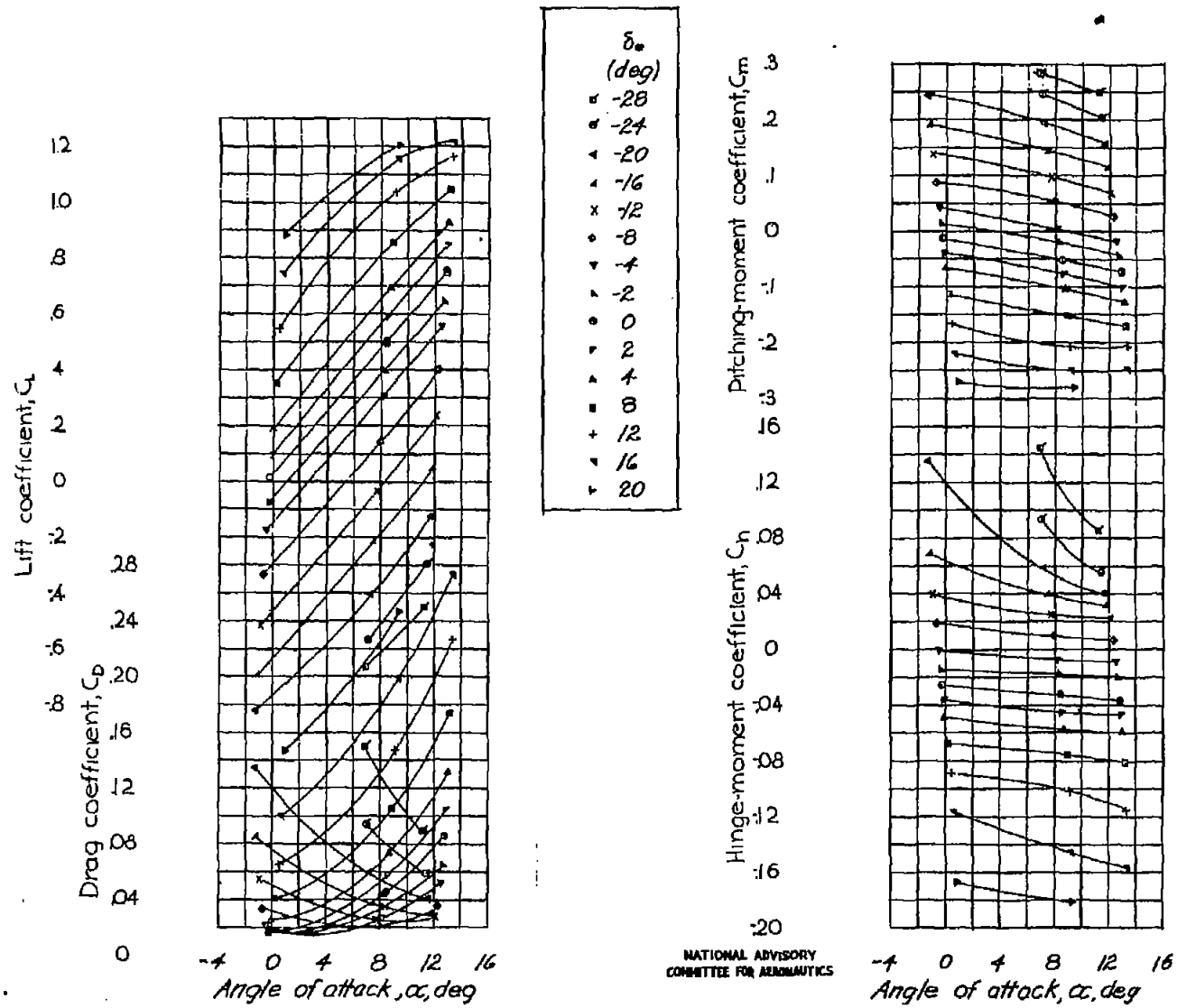

Figure 20.- Aerodynamic characteristics of the 0.5-scale model of left horizontal tail surface. Modification C; horn 4; $\delta_t = 10^\circ$.

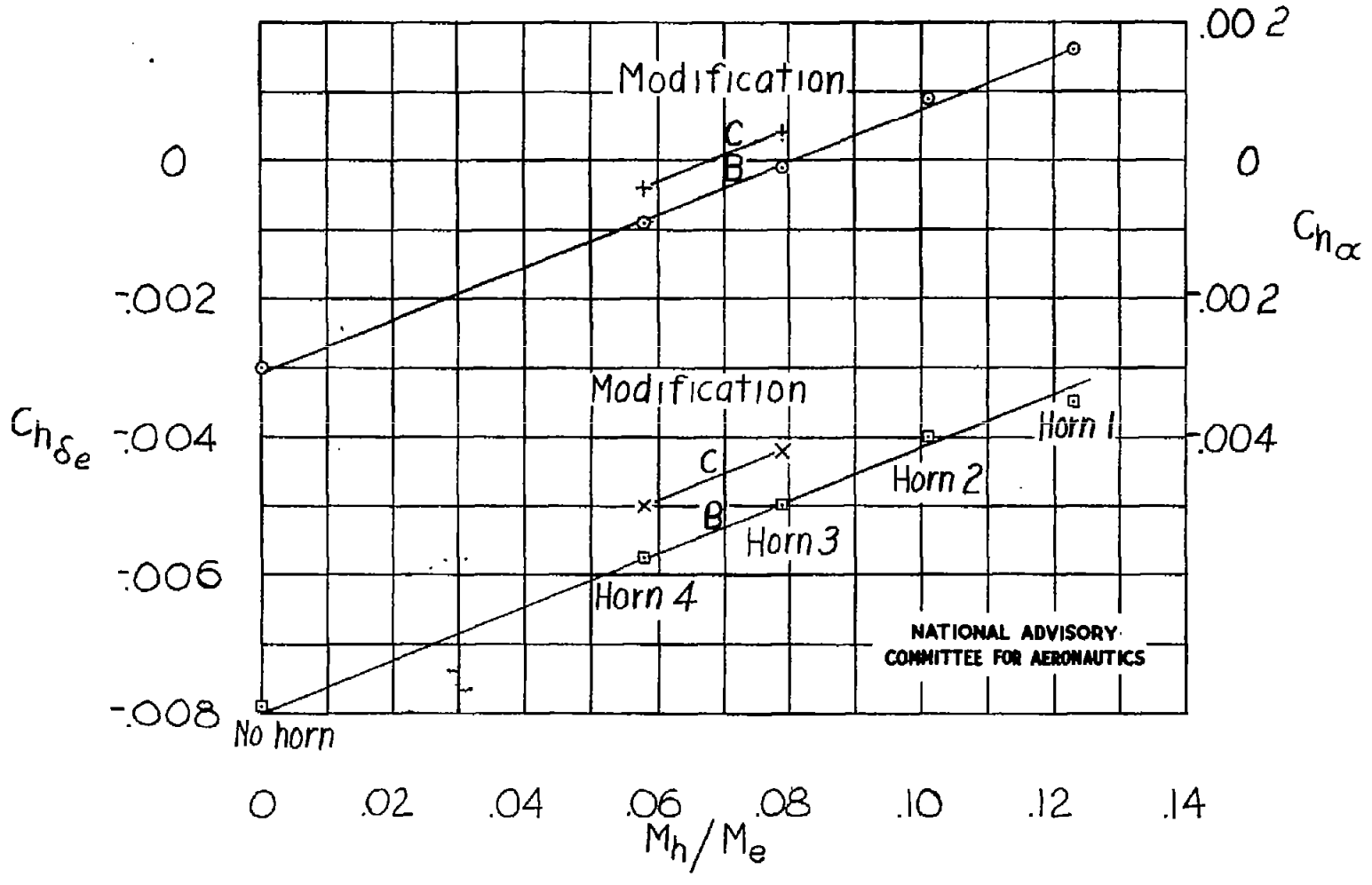

Figure 21.- Variation of hinge-moment parameters C_{h_α} and $C_{h_{\delta_e}}$ with ratio of horn area moment to elevator area moment.

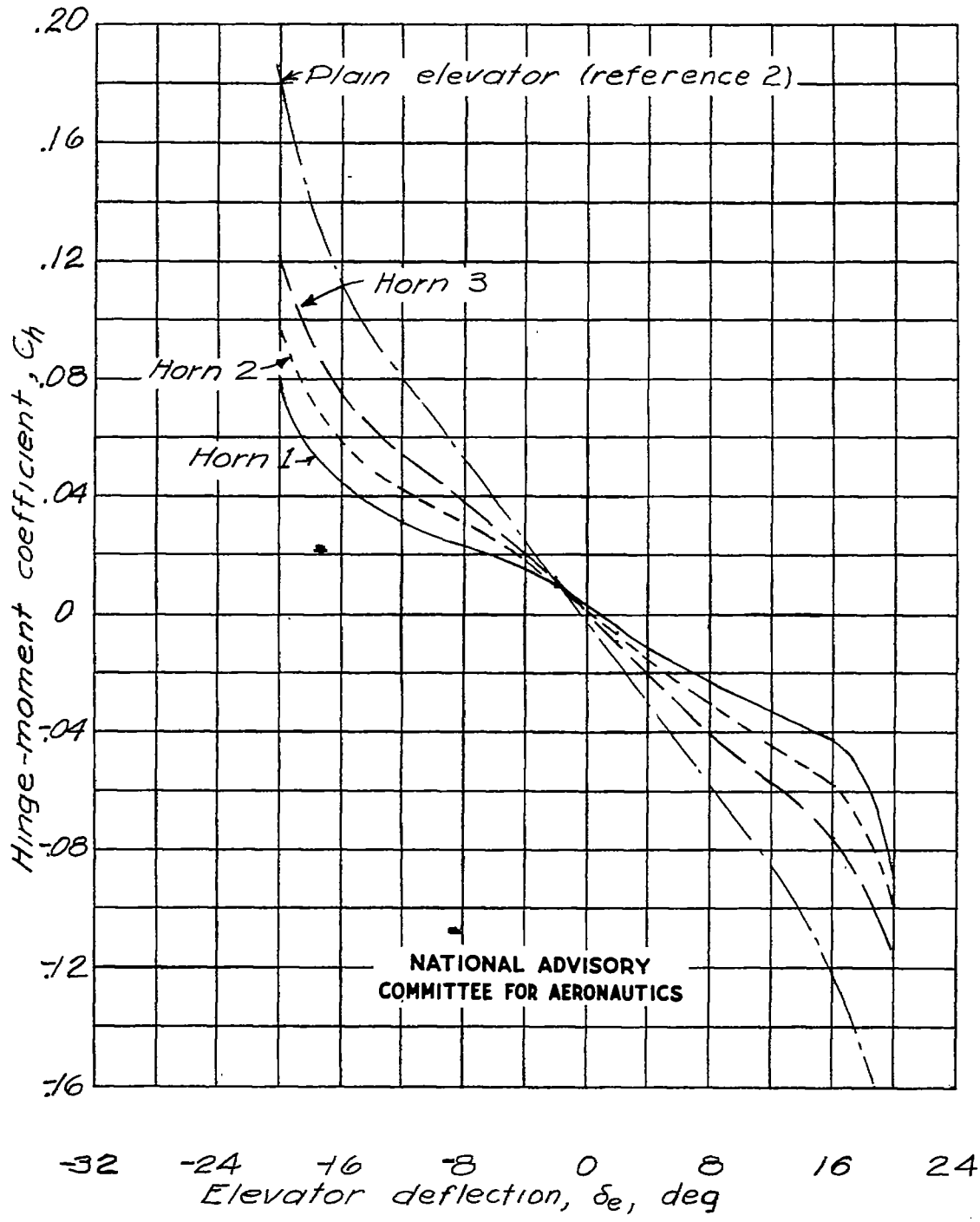

Figure 22.- Variation of hinge-moment coefficient with elevator deflection for plain (no horn) and balanced elevators.

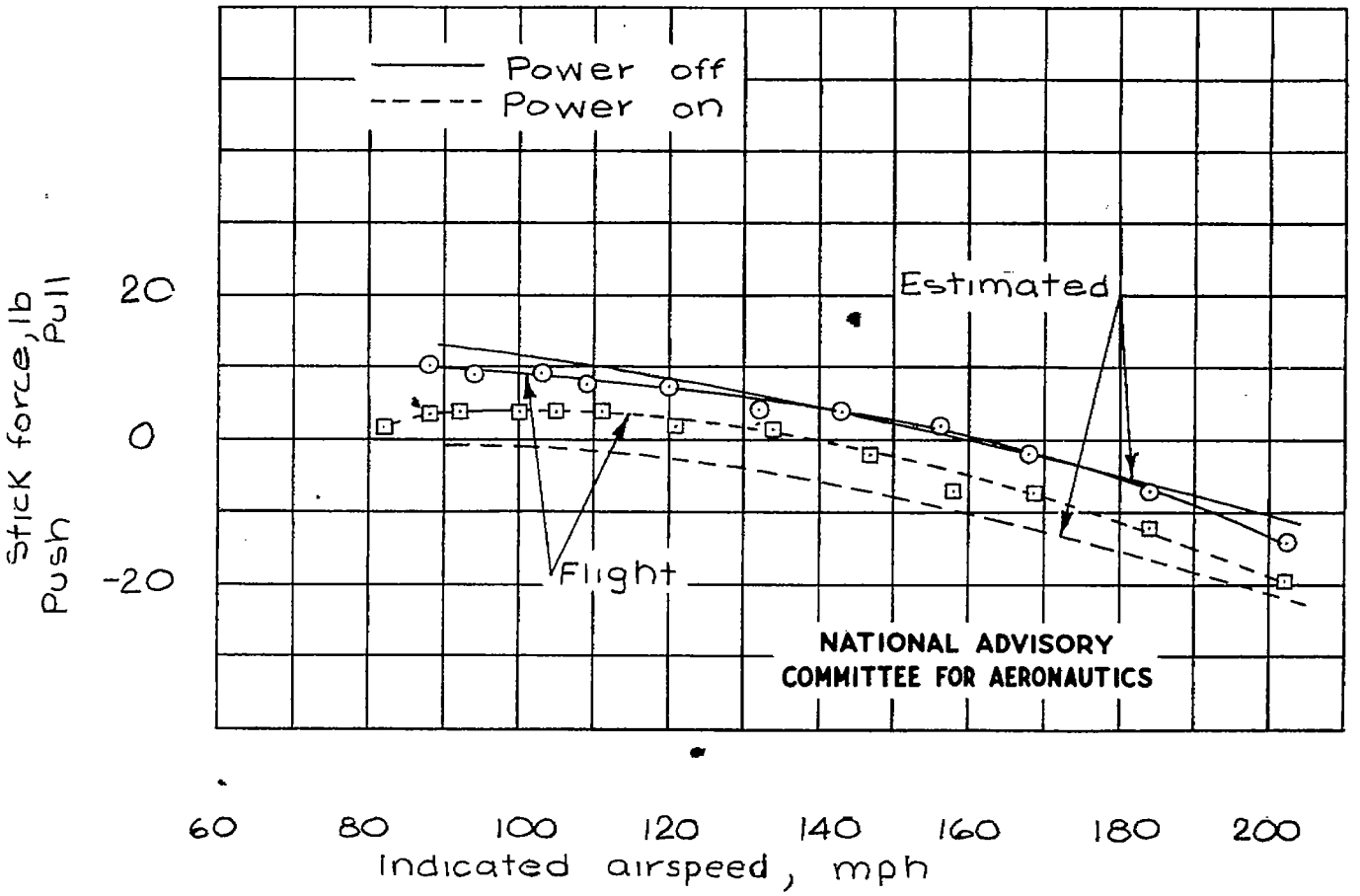

Figure 23.- Comparison of flight and estimated longitudinal trim characteristics of airplane tested. Center of gravity at 25.5-percent mean aerodynamic chord (wheels up); flap and landing gear up; $\frac{\delta_t}{\delta_e} = -0.5$; modification C; horn 3.